Eur. Phys. J. D **37**, 141–150 (2006)
DOI: 10.1140/epjd/e2005-00271-9

THE EUROPEAN PHYSICAL JOURNAL D

Qudit state estimation with a fixed set of bases

T. Bschorr[a], S. Probst-Schendzielorz, and M. Freyberger

Abteilung Quantenphysik, University Ulm, 89069 Ulm, Germany

Received 14 July 2005
Published online 4 October 2005 –

Abstract. We analyse the estimation of a pure d-dimensional quantum state with a finite number of measurements and compare several estimation schemes. In this paper we concentrate on consecutive von Neumann measurements on a finite number of identically prepared systems in dimensions $d = 2$, $d = 4$ and $d = 8$. We propose two schemes with different types of fixed measurement directions. Inspired by integration theory our first approach uses the Halton sequence (a so-called quasi-Monte Carlo sequence) to obtain measurement directions ('sampling points') with high uniformity over the configuration space. Our second approach extends this idea and optimises the distribution of the measurement directions to yield a rather high fidelity in quantum state estimation. This optimisation results in a uniform distribution of the directions and large quantum distances between the directions. Furthermore we establish a link to mutually unbiased bases.

PACS. 03.65.Wj State reconstruction, quantum tomography – 02.70.Uu Applications of Monte Carlo methods

1 Introduction

In quantum physics the state vector of a system is the fundamental object which mathematically describes our complete knowledge about it [1]. Quantum state estimation [2–4] is the task of obtaining this state description for an unknown system. The essential boundary condition is that this system is only available in finitely many copies. In principle we can further distinguish between estimation of states in an infinite dimensional Hilbert space and states spanned in finite dimensions.

In our paper we focus on the finite dimensional case. A typical quantum estimation scenario uses a finite ensemble of N systems which are identically prepared in the same unknown quantum state. Characteristic properties of this state have to be found from measured frequencies. The schemes presented so far can be divided into two groups. Optimal extraction of quantum information is achieved by a collective measurement on the whole ensemble [5–10], whereas successive single-system measurements [11–15] on each of the N systems are more feasible for experimental realisation [13,16,17]. We will restrict our investigation to single-system measurements.

Besides this, different levels of a priori knowledge of the unknown quantum state can be considered. The most important distinction is the one between pure states, see [8,11,18–20], and mixed states, see [10,12,21–24]. Most of the mentioned works deal with qubit-like systems. The focus of this paper is to present an operational approach for finite resources, that is a finite amount of copies, which easily extends to higher dimensions. As the number of needed parameters to describe a mixed state increases quadratically with the dimension d, but only linearly for pure states, we restrict our investigations to the latter case. That is, we still use a considerable amount of a priori knowledge. However, the generalisation to mixed states is, in principle, straightforward.

2 Basic principles of quantum state estimation

Our *estimation process* consists of consecutive measurements of specific observables on a finite ensemble of d-level systems (qu*d*its). We assume that all of these systems are prepared in the same unknown quantum state $|\Psi\rangle$. From the measured frequencies one can infer the quantum states using suitable estimators. That is, the estimator provides us with a prescription to transform measured frequencies into the estimated quantum state.

In our scheme we only consider consecutive von Neumann measurements on single systems. This assumption basically reflects current experimental possibilities [13,16]. The corresponding orthonormal measurement basis for the νth system is denoted by $\{|\Pi_0^\nu\rangle, \ldots, |\Pi_{d-1}^\nu\rangle\}$ and the corresponding measurement outcome by Π^ν. A central question of the present paper is the appropriate a priori choice of a measurement basis which corresponds to the a priori choice of a specific observable. We will propose

[a] e-mail: Thorsten.Bschorr@uni-ulm.de

several methods which are suitable for higher dimensional systems.

From a limited set of measurement results it is in general impossible to get complete knowledge of an arbitrary (pure) quantum state. Therefore, in general, the result of our estimation process will be a density operator $\hat{\rho}^{\mathrm{est}}$. We then can ask, which *pure* state $|\Psi^{\mathrm{est}}\rangle$ is closest to $\hat{\rho}^{\mathrm{est}}$, that is we determine (up to a global phase)

$$\max_{\psi} \langle\psi|\,\hat{\rho}^{\mathrm{est}}\,|\psi\rangle = \left\langle\Psi^{\mathrm{est}}\right|\hat{\rho}^{\mathrm{est}}\left|\Psi^{\mathrm{est}}\right\rangle. \tag{1}$$

If we represent $\hat{\rho}^{\mathrm{est}}$ by its spectral decomposition it is clear, that $|\Psi^{\mathrm{est}}\rangle$ is the eigenvector corresponding to the largest eigenvalue of $\hat{\rho}^{\mathrm{est}}$.

To quantify the quality of a *single estimation process* we use the fidelity

$$F(\Psi^{\mathrm{est}}|\Psi) \equiv \left|\langle\Psi^{\mathrm{est}}|\Psi\rangle\right|^2, \tag{2}$$

that is the overlap of the estimated pure state with the unknown pure state.

In order to quantify the quality of an *estimation scheme* we have to average over all possible states to get a mean fidelity

$$\overline{F} = \int_{\Omega} \mathrm{d}\psi\, F(\Psi^{\mathrm{est}}|\psi), \tag{3}$$

in which $\int_{\Omega}\mathrm{d}\psi$ symbolically denotes the uniform integration over the complete state space Ω.

The optimal mean fidelity which requires a collective measurement[1] on all N systems in d dimensions is given by [9]

$$\overline{F}^{\mathrm{opt}} \equiv \frac{N+1}{N+d}. \tag{4}$$

We will compare the fidelities of our single-system measurements to this optimal boundary.

3 Notation

An essential ingredient of quantum state estimation is an appropriate parameterisation of the state

$$|\Psi\rangle = \sum_{i=0}^{d-1} c_i\,|i\rangle\,. \tag{5}$$

In the d-dimensional computational basis $\{|0\rangle,\ldots,|d-1\rangle\}$ the complex coefficients c_i are given by a set of $2d$ parameters. The normalisation $\sum_{i=0}^{d-1}|c_i|^2=1$ reduces this set by one parameter. Moreover, we cannot determine a global phase of $|\Psi\rangle$ and hence it is sufficient to parameterise $|\Psi\rangle$ by $2(d-1)$ values. In other words the Hilbert space of a d-dimensional system is the complex projective space $\mathbb{C}P^{d-1}$, which can be described using the Hurwitz parameterisation [26,27] (i.e. generalised spherical coordinates). Using $d-1$ angles $\theta_k \in [0,\pi/2]$ and $d-1$ angles $\phi_k \in [0,2\pi)$ for $k=1,2,\ldots,d-1$ we obtain

$$\begin{aligned}
c_0 &= \cos\theta_1\\
c_1 &= \sin\theta_1\cos\theta_2\,\mathrm{e}^{\mathrm{i}\phi_1}\\
&\vdots\\
c_{d-3} &= \sin\theta_1\sin\theta_2\cdots\cos\theta_{d-2}\,\mathrm{e}^{\mathrm{i}\phi_{d-3}}\\
c_{d-2} &= \sin\theta_1\sin\theta_2\cdots\sin\theta_{d-2}\cos\theta_{d-1}\,\mathrm{e}^{\mathrm{i}\phi_{d-2}}\\
c_{d-1} &= \sin\theta_1\sin\theta_2\cdots\sin\theta_{d-2}\sin\theta_{d-1}\,\mathrm{e}^{\mathrm{i}\phi_{d-1}}\,.
\end{aligned} \tag{6}$$

For uniform distribution over almost all of $\mathbb{C}P^{d-1}$ [27] we use the 'polar' angles ϕ_k with probability density $P(\phi_k)=1/(2\pi)$. The 'azimuthal' angles θ_k have to be taken in a nonuniform way using the probability density $P(\theta_k)=2k\cos(\theta_k)\sin(\theta_k)^{2k-1}$. In practice this can be realised by introducing an auxiliary random variable ξ_k which is uniformly distributed in $[0,1]$ and setting $\theta_k=\arcsin\left(\xi_k^{1/(2k)}\right)$. Note that for qubits ($d=2$) this parameterisation equals the well-known Bloch picture on a unit sphere with angles $2\theta_1$ and ϕ_1.

Averaging over the configuration space Ω which is needed in equation (3) to calculate the mean fidelity is described by the multi-dimensional integral

$$\int_{\Omega}\mathrm{d}\psi \equiv \frac{1}{\mathrm{Vol}(\Omega)}\prod_{k=1}^{d-1}\int_0^{\pi/2}\cos\theta_k(\sin\theta_k)^{2k-1}\mathrm{d}\theta_k\prod_{k=1}^{d-1}\int_0^{2\pi}\mathrm{d}\phi_k \tag{7}$$

with volume

$$\mathrm{Vol}(\Omega) = \frac{\pi^{d-1}}{(d-1)!}\,. \tag{8}$$

4 Estimators

We now focus on the problem how we can infer the underlying quantum state after N measurements. Let us assume that we have found the measurement result Π^{ν} corresponding to the projector $|\Pi^{\nu}\rangle\langle\Pi^{\nu}|$ for the νth, $\nu=1,\ldots,N$, measurement. An estimated quantum state, which is consistent with these results, is given by the sum of projectors

$$\hat{\rho}_N^{\mathrm{est},\Sigma} = \frac{1}{N}\sum_{\nu=1}^{N}|\Pi^{\nu}\rangle\langle\Pi^{\nu}|\,, \tag{9}$$

which is motivated by the classical mean. For a given set of measurement directions this estimator only accounts for the measured frequencies of the results. It can therefore be regarded as an *incoherent* superposition of the measurement results.

A method which in some sense takes into account that the measured values might stem from a coherent superposition is the maximum-likelihood (ML) ansatz [20,22,28–30]. Its central element is the likelihood functional which is maximised by the corresponding ML

[1] It turns out that for this collective measurement one needs in general the concept of POVM measurements [25].

estimate. A possible choice for a likelihood functional for the estimation of a pure state is the overlap

$$\mathcal{L}_N(\psi) = \prod_{\nu=1}^{N} |\langle \Pi^\nu | \psi \rangle|^2 \tag{10}$$

which represents the likelihood of the measurement sequence found for a given state $|\psi\rangle$. The estimated state is then obtained by maximising the likelihood functional

$$\max_{\psi} \mathcal{L}_N(\psi) \to \left| \Psi_N^{\text{est,ML}} \right\rangle . \tag{11}$$

Another physically motivated ansatz uses a probability distribution (PD) $w_N(\psi)$ over the configuration space Ω parameterised by $2(d-1)$ angles as described before. This probability distribution has to be constructed from the N measurement results. Then it represents the estimated state

$$\hat{\rho}_N^{\text{est,PD}} = \int_\Omega \mathrm{d}\psi \, w_N(\psi) \, |\psi\rangle\langle\psi| \tag{12}$$

with normalisation $\int_\Omega \mathrm{d}\psi \, w_N(\psi) = 1$. The probability distribution $w_N(\psi)$ develops iteratively from measurement to measurement [11]. Before the first measurement (a priori) we know nothing about the underlying state, that is we start with $w_0(\psi) \equiv 1/\operatorname{Vol}(\Omega)$ which yields $\hat{\rho}_0^{\text{est,PD}} = \frac{1}{d}\hat{1}$. To update our information that is to update the probability distribution after the νth measurement we use Bayes' rule [31]

$$w_\nu(\psi) = \mathcal{N} P(\psi|\Pi^\nu) w_{\nu-1}(\psi) \tag{13}$$

with normalisation factor $\mathcal{N}$. Here the conditioned probability

$$P(\psi|\Pi^\nu) \equiv \langle \psi | \, \Pi^\nu \, |\psi\rangle \tag{14}$$

clearly depends on the $2(d-1)$ angles, equation (6), since $|\psi\rangle$ can be parameterised in analogy to equation (5).

Among the mentioned estimators the PD estimator, equation (12), accumulates most information. Besides the location of the estimated state the probability distribution also contains information about the distribution of the measurement results (that is the width of the distribution). This is consistent with our numerical results presented in Section 6 which proof that the PD estimator yields the highest average fidelities. However, with increasing d it is more and more complicated to store and handle $w_N(\psi)$ in order to evaluate equation (12). In this cases we will use the ML estimator. The simple estimator $\hat{\rho}^{\text{est},\Sigma}$ is only presented for completeness as it only uses incoherent superpositions which do not pay attention to the quantum nature of the described measurements.

Note that all mentioned estimators assure physical results. Equations (9) and (12) are convex combinations of projectors and the result clearly is a density operator. In equation (11) we assure a physical result by writing and maximising the likelihood functional in terms of pure states.

5 Construction of measurement bases

As already stated in Section 2 all measurements of our estimation scheme are given by a set of N von Neumann measurements defined by the bases $\{|\Pi_0^1\rangle, \ldots, |\Pi_{d-1}^1\rangle\}$, …, $\{|\Pi_0^N\rangle, \ldots, |\Pi_{d-1}^N\rangle\}$. Alternatively we can assume N unitary operators $\hat{U}^{(\nu)}$, $\nu = 1, \ldots, N$, which, if applied on the computational basis $\{|0\rangle, \ldots, |d-1\rangle\}$, yield the appropriate measurement state,

$$|\Pi_k^\nu\rangle = \hat{U}^{(\nu)} |k\rangle . \tag{15}$$

If expressed in the computational basis the coefficients of these states are given by the columns of the corresponding unitary matrix

$$U_{l,k}^{(\nu)} \equiv \langle l | \, \hat{U}^{(\nu)} \, |k\rangle_{l=1\ldots d} . \tag{16}$$

We now consider different approaches to calculate our measurement bases. In principle they can be divided into two groups: adaptive and non-adaptive ones. In an adaptive scheme the next measurement depends on the previous measurement results whereas in non-adaptive schemes we use a set of fixed bases which are independent of the measurement outcomes.

In the following we restrict ourselves to non-adaptive schemes and propose two different types of (fixed) bases:

1. quasi-Monte Carlo (QMC) bases which are based on low-discrepancy sequences, see Section 5.2;
2. quantum large distance (QLD) bases which are generated by optimising the distribution of the bases, see Section 5.3.

To quantify the quality of a set of measurement bases we use the mean fidelity, equation (3). The results of the QMC and QLD schemes are compared to random measurement bases (RND) which are described in the next section.

5.1 Random bases

The random bases approach (RND) uses N unitary matrices with the elements $U_{l,k}^{(\nu)}$, equation (16), drawn from the circular unitary ensemble (CUE) to generate the measurement bases. As described in the previous section, the columns of each matrix allow us to construct the desired measurement projectors in the computational basis.

A random matrix from CUE is parameterised by d^2 real parameters. The explicit construction of a random CUE matrix is presented in Appendix A. As we can drop a global-phase factor for each matrix, we need only d^2-1 real parameters which can be written in terms of a vector $\tilde{\mathcal{P}}^\nu$ (see Eq. (24) in the appendix for an explicit representation). Furthermore, for each set of von Neumann measurements we can choose the basis state $|\Pi_0^\nu\rangle$ as reference state and drop $d-1$ relative phases for the other basis states $|\Pi_i^\nu\rangle$, $i > 0$. Therefore a minimal parameterisation would only need $d^2 - 1 - (d-1) = d(d-1)$ real parameters. However, we do not know such a parameterisation

in connection with CUE. Therefore, we use the d^2-1 dimensional parameter vector $\tilde{\mathcal{P}}^\nu$. Mathematically speaking this corresponds to a surjection from d^2-1 to d^2-d parameters which introduces correlations between the d^2-1 parameters.

A set of N measurement bases now can be seen as a set

$$\{\tilde{\mathcal{P}}^1,\ldots,\tilde{\mathcal{P}}^N\} \tag{17}$$

of (d^2-1)-dimensional points $\tilde{\mathcal{P}}^\nu$.

5.2 Quasi-Monte Carlo bases

Inspired by results from numerical integration theory [32] where low-discrepancy (also called quasi-Monte Carlo) sequences perform better than random schemes in the case of a finite number of points we also investigate their behaviour in generating random quantum bases.

A low-discrepancy sequence $\tilde{\mathcal{P}}^1,\ldots,\tilde{\mathcal{P}}^n,\ldots$ of dimensionality $D\equiv d^2-1$ with $\tilde{\mathcal{P}}^\nu\in[0,1]^{\otimes D}$ is a sequence with the property that for all n, the subsequence $\tilde{\mathcal{P}}^1,\ldots,\tilde{\mathcal{P}}^n$ is almost uniformly distributed and $\tilde{\mathcal{P}}^1,\ldots,\tilde{\mathcal{P}}^{n+1}$ is almost uniformly distributed as well. A strict mathematical definition using the so-called star discrepancy can, for example, be found in [33].

A set of N quasi-Monte Carlo measurement bases $\tilde{\mathcal{P}}^1,\ldots,\tilde{\mathcal{P}}^N$ can now be generated by using a low-discrepancy sequence of dimensionality D and length N. The representation of $\tilde{\mathcal{P}}^\nu$ in the computational basis is obtained with the help of equations (25) and (26) as well as the construction principles of a CUE-matrix and is denoted in the appendix. Because of this principle, the property of almost uniform distribution translates from the quasi-Monte Carlo sequence to the angles and to the matrices. We should therefore get a set of measurement bases which are more uniformly distributed in Hilbert space than the pure random approach. Hence, we expect that this set of measurement bases is, on average, superior in quantum estimation compared to the pure random one.

In this work we restrict ourself to the scrambled Halton sequence [33–35] as a low discrepancy sequence. The construction principles of this sequence are presented in Appendix B and yield a set of measurement bases, equation (17).

5.3 Quantum large distance bases

In this section we further extend the idea of N uniformly distributed bases of dimension d, $\{|\Pi_0^1\rangle,\ldots,|\Pi_{d-1}^1\rangle\},\ldots,\{|\Pi_0^N\rangle,\ldots,|\Pi_{d-1}^N\rangle\}$. Inspired by the ideas of Jones [18], we now 'distribute' the bases in such a way that the distance of neighbouring bases is as large as possible.

In a pictorial picture we may think of a measurement basis as being a 'spider' with d charged 'legs' representing the basis states. In order to ensure orthonormality of the basis states we think of the 'legs' being fixed to each other. Therefore, such a basis 'spider' can only evolve as a whole. In addition, all charges are equal. Our Hilbert space can be seen as 'inhabited' by N equally charged 'spiders' which try to avoid each other.

If the N measurement bases are 'distributed' in a uniform way we expect better performance, that is higher fidelity in quantum state estimation, because, on average, every unknown state $|\Psi\rangle$ has the same distance to the measurement projectors. Hence, we will scan $|\Psi\rangle$ quantum mechanically in a quite uniform way.

To achieve this, we start with N randomly oriented bases (generated, for example, by the RND method, see Sect. 5.1). We then simulate dynamic evolution of the system with a 'repelling force' inversely proportional to the square of the distance $d(\Pi_i^\nu,\Pi_j^\mu)^2$ between two basis states $|\Pi_i^\nu\rangle$ and $|\Pi_j^\mu\rangle$ of two different bases, $\nu\neq\mu$. For this work we have only used the Bures distance [36,37]

$$d_{\mathrm{B}}(\Pi_i^\nu,\Pi_j^\mu)^2=2(1-|\langle\Pi_i^\nu|\Pi_j^\mu\rangle|)\,, \tag{18}$$

to simulate the dynamic evolution, but other definitions like the Fubini-Study distance [37] $d_{\mathrm{FS}}(\Pi_i^\nu,\Pi_j^\mu)=\arccos|\langle\Pi_i^\nu|\Pi_j^\mu\rangle|$ are also possible.

The evolution is approximated in the following way. We start by calculating the force acting on $|\Pi_0^1\rangle$ by the states $|\Pi_j^\nu\rangle$ with $\nu>1$ and $j=0,\ldots,d-1$. We have examined two ways of expressing this force. An obvious approach is to represent the state

$$|\Pi_0^1\rangle\equiv|\Pi_0^1(\boldsymbol{\mathcal{X}}_0^1)\rangle=|\Pi_0^1(\theta_1,\ldots,\theta_{d-1},\phi_1,\ldots,\phi_{d-1})\rangle \tag{19}$$

in the computational basis using the generalised coordinates

$$(\boldsymbol{\mathcal{X}}_0^1)\equiv(\theta_1,\ldots,\theta_{d-1},\phi_1,\ldots,\phi_{d-1}) \tag{20}$$

introduced in equation (6). For a first approach we ignore the underlying Fubini-Study metric [38] and treat $\theta_1,\ldots,\theta_{d-1}$ and $\phi_1,\ldots,\phi_{d-1}$ like Euclidean coordinates. With this approximation the evolution starting from rest can be written as

$$\boldsymbol{\mathcal{X}}_0^{1\prime}=\boldsymbol{\mathcal{X}}_0^1+\frac{1}{2}(\Delta t)^2\sum_{\nu=2}^{N}\sum_{j=0}^{d-1}\frac{1}{d_{\mathrm{B}}(\boldsymbol{\mathcal{X}}_0^1,\boldsymbol{\mathcal{X}}_j^\nu)^2}\frac{\boldsymbol{\mathcal{X}}_0^1-\boldsymbol{\mathcal{X}}_j^\nu}{d_{\mathrm{B}}(\boldsymbol{\mathcal{X}}_0^1,\boldsymbol{\mathcal{X}}_j^\nu)} \tag{21}$$

with $d_{\mathrm{B}}(\boldsymbol{\mathcal{X}}_0^1,\boldsymbol{\mathcal{X}}_j^\nu)$ being the distance defined in equation (18) and expressed by the coordinates of equation (6). After a small time step Δt we use Gram-Schmidt orthonormalisation to get the new (rotated) basis $\left\{\left|\tilde{\Pi}_0^1\right\rangle,\ldots,\left|\tilde{\Pi}_{d-1}^1\right\rangle\right\}$. For simplicity, we start every step from rest[2]. We then calculate the action of the states $|\Pi_i^\nu\rangle$, $\nu\neq2$ on $|\Pi_0^2\rangle$ in an analogous way. After orthonormalisation we then obtain $\left\{\left|\tilde{\Pi}_0^2\right\rangle,\ldots,\left|\tilde{\Pi}_{d-1}^2\right\rangle\right\}$. This procedure is repeated for all bases. After all N measurement bases have undergone a time step we repeat the whole procedure. In order to randomise the orthogonalisation which

[2] Of course, the evolution can also be done including a first time derivative of $\boldsymbol{\mathcal{X}}_0^1$ in every step, but besides changing the convergence rate we have confirmed that it does not change the result of the evolution.

is always performed in increasing index-ordering and to apply the action of the repulsion on a different state of the basis we permute the indices of the states of each basis before repeating. We stop the evolution if we reach an equilibrium, that is at one step the absolute value of all 'forces' is below some limit. If the procedure does not converge we stop after a predetermined amount of iterations.

If the iteration converges our bases are oriented in such a way that the (nearest) neighbour distance of each of the $N \times d$ states in Hilbert space tends to a (local) maximum. If the iteration does not converge we end up with a somehow partially optimised set. Nevertheless, we expect that this distribution is considerably better than random.

The second possibility of implementing the evolution is to write $\left|\Pi_0^1\right\rangle$ in terms of its coefficients in the computational basis, see equation (5), and treat the coefficients as independent coordinates. Note that in this approach a time step implemented analogously to equation (21) generates a non-normalised state which must be re-normalised before re-orthogonalisation of the bases.

A further possibility to obtain an equilibrium distribution of our measurement bases would be to calculate a global potential measure like $\sum_{\nu\neq\mu}\sum_{i,j=1}^{d}\left(d_{\mathrm{B}}(\Pi_i^\nu,\Pi_j^\mu)\right)^{-1}$ for all quantum distances and then use numerical minimisation. The difficulty here is the large number $N\times(d^2-1)$ of parameters for higher dimensions. The quantum correlation information (Kullback information) is another possible global quantity [18].

5.3.1 QLD bases and MUB

In the following we establish a connection between our QLD bases and mutually unbiased bases (MUB) [39–41].

Two d-dimensional orthonormal bases $\{|\Pi_0\rangle,\ldots,|\Pi_{d-1}\rangle\}$ and $\{|\Pi_0'\rangle,\ldots,\left|\Pi_{d-1}'\right\rangle\}$ are MUB if and only if $\left|\langle\Pi_i|\Pi_j'\rangle\right|^2=\frac{1}{d}$, for every $i,j=0,\ldots,d-1$. It is known that if the dimension d is a prime power, sets with at most $d+1$ pairwise MUB exist [40,41].

A consequence of equation (18) is that maximisation of the distance between $|\Pi_i\rangle$ and $\left|\Pi_j'\right\rangle$ corresponds to minimising the overlap $\left|\langle\Pi_i|\Pi_j'\rangle\right|^2$. In the QLD ansatz we want to minimise this overlap for all $i,j=0,\ldots,d-1$. Normalisation

$$1=\langle\Pi_i|\Pi_i\rangle=\sum_{j=0}^{d-1}\left|\langle\Pi_i|\Pi_j'\rangle\right|^2 \tag{22}$$

implies that this is achieved by $\left|\langle\Pi_i|\Pi_j'\rangle\right|^2=\frac{1}{d}$. A set of MUB is therefore always a set of QLD bases.

For dimensions $d\in\{2,3,4,5\}$ our algorithms produce sets of $N\leq d+1$ MUB[3]. For higher (prime power) values of d our numerical approaches do not converge to a set of $N\leq d+1$ MUB. The reason for this may be the two approximations in our dynamic description as described in Section 5.3. First, we perform dynamical evolution only on one basis vector represented by $\boldsymbol{\mathcal{X}}_0^\nu$, equation (20), and re-orthogonalise the basis afterwards instead of rotating the complete basis. Second, we simplify the calculation by assuming an Euclidean coordinate space. The mentioned ansatz with a global potential avoids the first approximation, but again we do not consider the proper metric.

[3] The numerical value of $\left|\left|\langle\Pi_i|\Pi_j'\rangle\right|^2-\frac{1}{d}\right|$ is always less than 10^{-5}.

5.3.2 Visualisation of QLD bases for d = 2

In the 2-dimensional case the QLD bases can be visualised using the Bloch-vector picture with angles $2\theta_1$ and ϕ_1. A measurement basis consists of two antipodal points on the Bloch sphere. Or in a pictorial view, it is a barbell.

For $N=2$ and $N=3$ the corresponding barbells are pairwise perpendicular to each other resulting in a maximal distance of $\sqrt{2}$ for neighbouring points. In the case of $N=4$ bases the situation is more complicated. It turns out that the QLD bases align with the centres of the faces of a regular octahedron (with opposite faces forming a basis). The nearest neighbour distance of this configuration is equal to $\sqrt{4/3}$. For $N=6$ we can again use a Platonic solid to visualise the QLD bases [18]. The centres of the faces of a regular dodecahedron or, equivalently, the corners of an icosahedron, have a nearest neighbour distance of $4/\sqrt{2(5+\sqrt{5})}$. The values of these geometrical results and our numerical optimisation agree perfectly.

In principle, this geometrical picture could also be extended to higher dimensions. However, for $d>2$ the Bloch-vector picture is more complicated for visualisation [42,43].

5.4 Discussion

To clarify the different properties concerning uniformity of our bases we give an example for the distribution of the measurement bases in dimension $d=2$. The Hilbert space is again visualised using the Bloch sphere with angles $2\theta_1$ and ϕ_1. Figure 1 shows the distribution for $N=8$ measurement bases. The metric is incorporated by plotting the points in $(\cos 2\theta_1-\phi_1)$-space.

In the shown example the QMC approach is clearly distributed in a more uniform way than the RND ansatz. But, for example, the points with symbols '$\times$' and '$\square$' are very close to each other. This is due to the non-optimal parameterisation mentioned in Section 5.2.

The QLD approach clearly results in the most uniform distribution of the bases. The pattern of the symbols is quite regular.

6 Numerical simulations

In this section we present Monte Carlo simulations for the different estimation scenarios. A scenario is defined by choosing a certain estimator (Sect. 4) and a measurement basis (Sect. 5). Our main issue is to bring out the

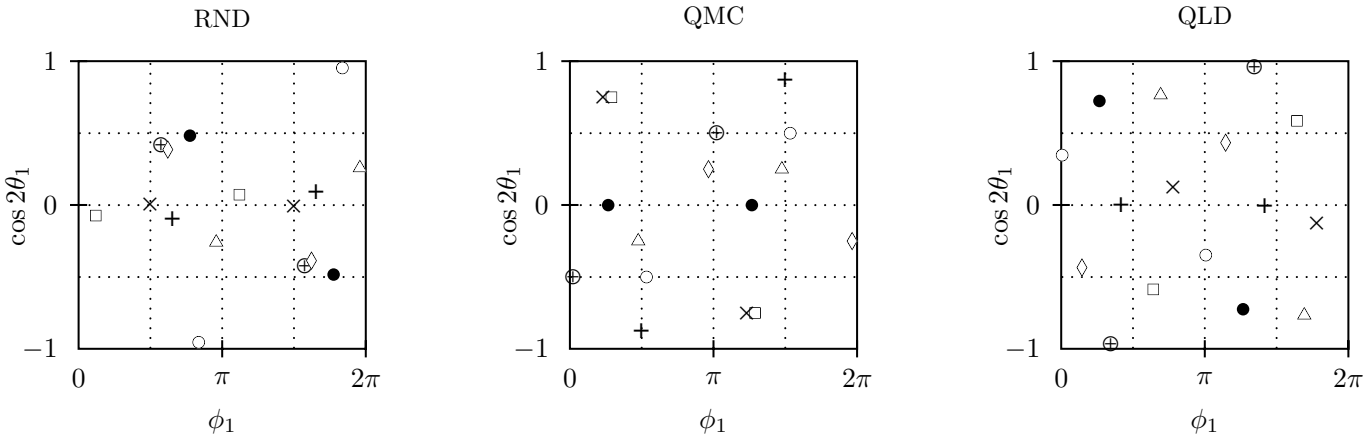

Fig. 1. The plots show $N = 8$ measurement bases for qubits ($d = 2$) on the Bloch sphere, which is represented in $(\cos 2\theta_1 - \phi_1)$-space. Each measurement base is given by two antipodal points on the sphere. Each pair of antipodal points is depicted with the same symbol. From left to right we show the RND, QMC and QLD ansatz for a single run. We can clearly see the uniformity of the QLD approach.

performance of the desired measurement bases for increasing dimensionality d. Hence we do not present results for all possible estimators. We restrict ourselves to the probability distribution (PD) estimator for $d = 2$ and $d = 4$. As the probability-distribution ansatz, equation (12), is very time-consuming for higher dimensions, we use the maximum-likelihood (ML) ansatz for $d = 8$. For all these cases we compare the average fidelity $\overline{F}$, equation (3) to the optimal fidelity $\overline{F}^{\mathrm{opt}}$, equation (4), as a function of the finite ensemble size N.

6.1 Principles of the simulation

The average fidelity $\overline{F}$, equation (3), is approximated by Monte Carlo averaging over M (typically 10^5 to 10^6) single-run fidelities F_μ defined according to equation (2),

$$\overline{F} = \frac{1}{M} \sum_{\mu=1}^{M} F_\mu. \tag{23}$$

For each single run we randomly choose an unknown state[4] $|\Psi\rangle$, equation (5), and calculate the estimated state $|\Psi^{\mathrm{est}}\rangle$ as discussed in Section 4.

In case of the probability distribution estimator $\hat{\rho}^{\mathrm{est,PD}}$, equation (12), the integration is evaluated by expressing the probability distribution $w_N(\psi)$, equation (13), in terms of sine and cosine functions of the angles θ_k and ϕ_k. The integration can then be performed term by term with the help of beta functions. It requires d terms to express a general probability in the computational basis. Hence, the number of terms grows exponentially with the amount of used resources. Therefore, this approach is only applicable for $d = 2$ or $d = 4$ and a small number of resources N.

Instead of evaluating the integral, equation (12), term by term one can also use numerical integration[5]. Instead of dealing with a huge number of terms we have to deal with exponentially growing integration space which increases the number of needed points to achieve a given accuracy.

The maximisation needed to evaluate the maximum-likelihood estimator $\hat{\rho}^{\mathrm{est,ML}}$, equation (11), is performed numerically [44].

6.2 Qubits, d = 2

We start with the simplest case, namely two-level systems.

In Figure 2 we present the ratio $\overline{F}^{\mathrm{PD}}/\overline{F}^{\mathrm{opt}}$ evaluated with the probability-distribution estimator $\hat{\rho}^{\mathrm{est,PD}}$, equation (12), and the optimal fidelity $\overline{F}^{\mathrm{opt}}$, equation (4). We compare randomly chosen (RND) bases (see Sect. 5.1), quasi-Monte Carlo (QMC) bases (see Sect. 5.2) and quantum large distance (QLD) bases (see Sect. 5.3). We have chosen the probability-distribution estimator because it yields the highest average fidelity of all described estimators and it can still be treated numerically for $d = 2$.

We can clearly see the advantage of the QMC bases over the random basis. We can also see that for some numbers N of resources the Halton set performs better (that is, yields a higher fidelity) than for others. We do not know the exact cause of this oscillations as it is a mixture of the parameter-dimensionality mismatch discussed in Section 5.1 and peculiarities of the chosen quasi-Monte Carlo sequence (scrambled Halton sequence). With increasing N the QMC bases approach the QLD bases, which deliver the best values. However, the effort to calculate the QLD bases is much higher (expressed in the number of performed calculations, i.e. runtime). For $N \lessapprox 15$ the effort for the QLD ansatz pays off, but for a larger amount of quantum resources the QMC ansatz only has minor losses in the average fidelity.

[4] For randomly chosen states the QMC and QLD schemes are unbiased.

[5] The sampling points are generated using quasi-Monte Carlo methods [32].

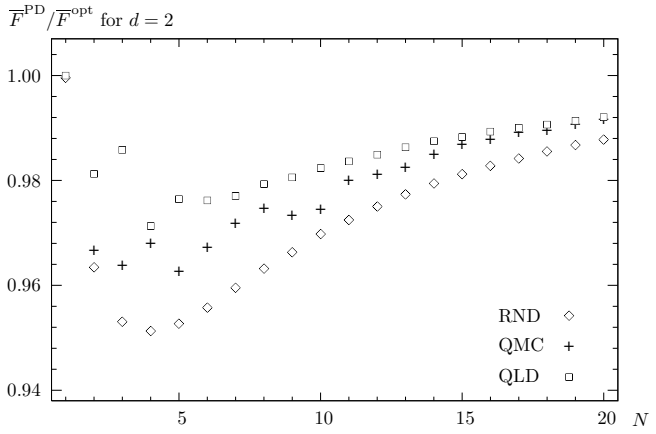

Fig. 2. The plot shows $\overline{F}^{\mathrm{PD}}/\overline{F}^{\mathrm{opt}}$ (for $d = 2$) as a function of the total number N of measurements (which equals the number of resources) for different measurement bases. The averaging was done by 10^6 Monte Carlo runs. The numerical error bars for a 2σ confidence interval are smaller than the symbols used to plot the data points. The QLD bases ($\square$) yield the best performance. The QMC choice ($+$) is better than the random choice ($\diamond$) albeit it is less smooth. One reason for this is the non-optimal parameterisation, see Section 5.1. For larger values of N it is easier (in terms of runtime) to calculate the QMC-bases compared to the QLD bases and the average fidelity of these two cases only slightly differs: QMC is "cheap and good".

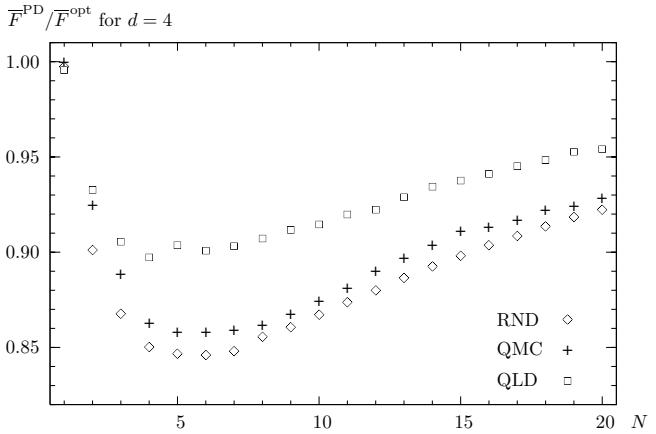

Fig. 3. In analogy to Figure 2 we present $\overline{F}^{\mathrm{PD}}/\overline{F}^{\mathrm{opt}}$ for $d = 4$. The data were obtained by averaging over 25×10^3 Monte Carlo runs for each number N of measurements. Due to the complexity of evaluating the integral the data set consists of a smaller number of runs which results in larger error bars (the omitted 2σ confidence interval is still about the size of the symbols). The qualitative behaviour is as in the qubit-case. The QMC curve ($+$) is more smooth and shows only a small benefit in comparison to the random curve ($\diamond$). Our QLD approach ($\square$) again yields the highest fidelity. The small spike for $N = 5$ is a consequence of the estimation using mutually unbiased bases.

Note that by introducing adaptive measurements [11] one can obtain $\overline{F}$ values close to the optimum $\overline{F}^{\mathrm{opt}}$, equation (4). For qubits this optimisation is feasible, but for higher dimensional systems (on which we want to set our focus) it is very hard. Besides this, for $1 \leq N \leq 20$ the adaptive scheme yields at most 1% higher fidelity than our QLD scheme, but for higher dimensions the situation may be different. However, in this paper we focus on relatively simple estimation schemes based on a fixed set of measurement operators.

Note also that the average fidelity $\overline{F}$ is a monotonic increasing function of N. Despite this, the ratio $\overline{F}/\overline{F}^{\mathrm{opt}}$ is, in general, a non-monotonic function because the different fidelities scale differently for increasing N.

We further mention that for $N = d + 1 = 3$ our QLD bases form a maximal set of MUB (see Sect. 5.4) which explains the good performance in this case.

6.3 Qudits, d = 4

For $d = 4$ (two qubits) the probability distribution estimator $\hat{\rho}^{\mathrm{est,PD}}$, equation (12), is already hard to calculate. Due to the exponentially growing number of terms in the beta-function evaluation, we use numerical integration to evaluate $\overline{F}^{\mathrm{PD}}$, equation (3).

Again, the quasi-Monte Carlo bases perform better than the pure random choice. Compared to $d = 2$ the benefit is, however, much smaller. This is due to the mentioned correlations in our parameterisation. In two dimensions the effect was small but this will not be the case for higher dimensions. The QLD bases again yield the best estimation. For $N = d + 1 = 5$ our QLD bases form a maximal set of MUB which results in a small peak of $\overline{F}^{\mathrm{PD}}/\overline{F}^{\mathrm{opt}}$ (see Fig. 3).

6.4 Qudits, d = 8

As the evaluation of the integrals for the PD estimator $\hat{\rho}^{\mathrm{est,PD}}$, equation (12), turns out to be very extensive already for $d = 4$, we restrict our analysis for three qubits ($d = 8$) to the maximum-likelihood estimator $\hat{\rho}^{\mathrm{est,ML}}$, equation (11). The corresponding results of our simulations are shown in Figure 4. The QMC bases yield only a very small benefit in comparison to the RND ansatz. Using other low-discrepancy sequences [33] may increase the benefit. We have also analysed the Hammersley sequence [33,45], which is quite similar to the Halton sequence, and did not observe considerable changes. But, so far, we did not investigate other sequences. Therefore, the dominant reason for the small benefit may be again the previously mentioned mismatch in parameter dimensions. As in the other cases, the QLD bases again yield the best estimation. Due to the approximations in the construction of the QLD bases (see Sect. 5.3.1), we do not see the MUB-peak for $N = d + 1 = 9$ resources. Nevertheless the QLD ansatz performs considerably better than RND and QMC.

To get an idea of the closeness of our QLD bases for $N = 9$ resources we have compared it to the MUB given by Lawrence et al. in [46]. Averaged over 10^6 Monte Carlo

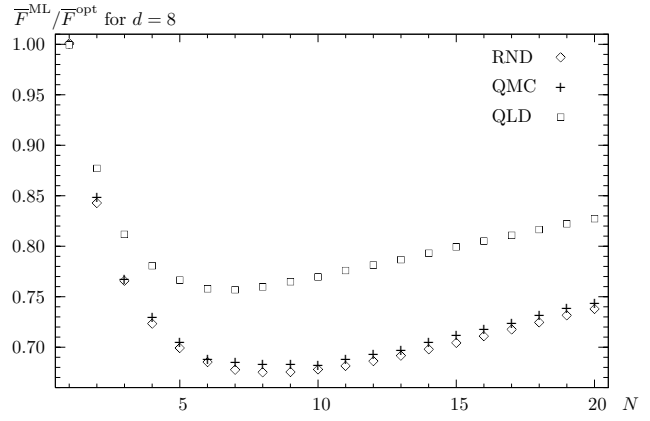

Fig. 4. $\overline{F}^{\mathrm{ML}}/\overline{F}^{\mathrm{opt}}$ for $d = 8$ evaluated with 10^6 Monte Carlo runs. Our QMC ansatz (+) only yields a very small enhancement compared to the random case (RND, $\diamond$) while the distributed bases (QLD, $\square$) enhances the estimation fidelity.

runs the MUB yield about 1.8% higher fidelity than our QLD optimisation.

As an interesting remark we mention that in the QLD case the simple projector-sum estimator $\hat{\rho}^{\mathrm{est},\Sigma}$, equation (9), yields slightly higher average fidelities $\overline{F}$ than the maximum-likelihood estimator, equation (11). This is due to the high uniformity of the QLD bases. This indicates that the chosen likelihood function, equation (10), may not be the best choice for the quantum state estimation task. As the intention of this paper are the different measurement bases we do not further address this question here.

7 Conclusions

In this paper we have investigated quantum state estimation for higher dimensions. We have presented and compared several ways of generating a fixed set of measurement bases. Our main aspect is the concept of Quantum Large Distances (QLD) which in some sense is similar to ideas presented by Jones in 1991 [18]. The QLD ansatz distributes the measurement bases in such a way in the configuration space that the Hilbert space is uniformly covered. We achieve this by maximising the (nearest) neighbour distance of the states describing the measurement. Another ansatz to obtain a set of measurement bases is the use of the circular unitary ensemble (CUE). We have examined two ways of generating the CUE. Using random numbers (RND) and, on the other hand, using quasi Monte Carlo (low-discrepancy) sequences (QMC).

In addition we have given different approaches for quantum estimators. As the intention of this paper is the construction of measurement bases, we have, however, not presented a detailed analysis about this topic. Depending on the dimensionality, we have used the most suitable one for each case.

We have numerically compared the average fidelities $\overline{F}$ and the optimal fidelity $\overline{F}^{\mathrm{opt}}$ for $d = 2$, $d = 4$ and $d = 8$ for different amounts N of finite resources. The QLD ansatz is always superior to the CUE bases approaches RND and QMC. Of course, in the limit $N \to \infty$ they asymptotically reach the optimal value $\overline{F}^{\mathrm{opt}}$.

As the dimensionality increases the average fidelity for the QMC bases and the RND bases become very close. For $d = 8$ the difference is only minor, whereas for $d = 2$ the QMC ansatz yields a clear improvement. In terms of complexity the QMC method requires only marginal additional effort compared to RND. In contrast, the QLD method requires considerably more effort than RND but yields a clear improvement of the average fidelity. And, as noted in the previous section, due to its uniformity it can also be evaluated using the simplest estimator $\rho^{\mathrm{est},\Sigma}$, equation (9).

We acknowledge financial support by the Deutsche Forschungsgemeinschaft within the *Schwerpunktprogramm Quanten-Informationsverarbeitung* (SPP1078) and by the European Commission network CONQUEST.

Appendix A: Circular unitary ensemble

According to [26,47] a parameterisation of CUE can be obtained by decomposing the unitary matrix $U = (U_{l,k})$, equation (16), into the elementary operations of two-dimensional subspaces $E^{(i,j)}(\phi, \psi, \chi)$ with non-zero elements

$$\begin{aligned}
&(E^{(i,j)})_{kk} = 1, \qquad k = 1, \ldots, d, \quad k \neq i, j \\
&(E^{(i,j)})_{ii} = \cos\phi \; \mathrm{e}^{\mathrm{i}\psi}, \qquad (E^{(i,j)})_{ij} = \sin\phi \; \mathrm{e}^{\mathrm{i}\chi} \\
&(E^{(i,j)})_{ji} = -\sin\phi \; \mathrm{e}^{-\mathrm{i}\chi}, \; (E^{(i,j)})_{jj} = \cos\phi \; \mathrm{e}^{-\mathrm{i}\psi}.
\end{aligned}$$

With the help of the composite rotations

$$\begin{aligned}
E_1 &= E^{(1,2)}(\phi_{1,2}, \psi_{1,2}, \chi_{1,2}) \\
E_2 &= E^{(2,3)}(\phi_{2,3}, \psi_{2,3}, 0) E^{(1,3)}(\phi_{1,3}, \psi_{1,3}, \chi_{1,3}) \\
E_3 &= E^{(3,4)}(\phi_{3,4}, \psi_{3,4}, 0) E^{(2,4)}(\phi_{2,4}, \psi_{2,4}, 0) \\
&\quad \times E^{(1,4)}(\phi_{1,4}, \psi_{1,4}, \chi_{1,4}) \\
&\vdots \\
E_{d-1} &= E^{(d-1,d)}(\phi_{d-1,d}, \psi_{d-1,d}, 0) \\
&\quad \times E^{(d-2,d)}(\phi_{d-2,d}, \psi_{d-2,d}, 0) \\
&\quad \times \cdots \times E^{(1,d)}(\phi_{1,d}, \psi_{1,d}, \chi_{1,d}),
\end{aligned}$$

a general unitary matrix is then described by $U = \mathrm{e}^{\mathrm{i}\alpha} E_1 E_2 \ldots E_{d-1}$.

Every transformation E_i appears once and only once. If we restrict $\phi_{r,s}$ to the interval $[0, \frac{\pi}{2}]$ and choose $\psi_{r,s}$, $\chi_{1,s}$ and α from $[0, 2\pi)$ we have found a parameterisation of a matrix U drawn from CUE in terms of the $d^2 - 1$ dimensional parameter vector

$$\begin{aligned}
\mathcal{P} = \big(&\phi_{1,2}, \ldots, \phi_{1,d}, \phi_{2,3}, \ldots, \phi_{2,d}, \ldots \phi_{d-1,d}, \\
&\psi_{1,2}, \ldots, \psi_{1,d}, \psi_{2,3}, \ldots, \psi_{2,d}, \ldots \psi_{d-1,d}, \\
&\chi_{1,2}, \ldots, \chi_{1,d}\big)
\end{aligned} \tag{24}$$

and the global phase α.

A uniform distribution[6] of the matrices can be obtained by introducing auxiliary random variables $\tilde{\phi}_{r,s}$, $\tilde{\psi}_{r,s}$, $\tilde{\chi}_{1,s}$ and $\tilde{\alpha}$ which are uniformly distributed in the interval $[0,1]$ and setting

$$\begin{aligned} \phi_{r,s} &= \arcsin\left((\tilde{\phi}_{r,s})^{1/2r}\right), \ \psi_{r,s} = 2\pi\tilde{\psi}_{r,s}\,, \\ \chi_{1,s} &= 2\pi\tilde{\chi}_{1,s}\,, \qquad\qquad \alpha = 2\pi\tilde{\alpha}\,. \end{aligned} \tag{25}$$

For our purposes we can always choose $\tilde{\alpha} \equiv 0$ as its only effect is multiplication of every basis state by a constant phase, which cancels out in the corresponding measurement projectors. Then

$$\begin{aligned} \tilde{\mathcal{P}} = \big(&\tilde{\phi}_{1,2},\ldots,\tilde{\phi}_{1,d},\tilde{\phi}_{2,3},\ldots,\tilde{\phi}_{2,d},\ldots\tilde{\phi}_{d-1,d}, \\ &\tilde{\psi}_{1,2},\ldots,\tilde{\psi}_{1,d},\tilde{\psi}_{2,3},\ldots,\tilde{\psi}_{2,d},\ldots\tilde{\psi}_{d-1,d}, \\ &\tilde{\chi}_{1,2},\ldots,\tilde{\chi}_{1,d}\big) \end{aligned} \tag{26}$$

defines a point in the d^2-1 dimensional unit-cube which characterises a random matrix drawn from CUE.

Appendix B: The scrambled Halton sequence

A key ingredient to calculate the points of the Halton sequence [33,34] is the b-adic representation of the integer number

$$\nu = \sum_{k=0}^{\infty} \alpha_k b^k\,,\ \alpha_k \in \{0,\ldots,b-1\}\,. \tag{27}$$

The radical inverse function of ν to the basis b is then defined as

$$\Phi_b(\nu) = \sum_{k=0}^{\infty} \alpha_k b^{-k-1} \tag{28}$$

and has the effect of mirroring the b-adic representation of ν, equation (27), at the decimal point, e.g. $\Phi_{10}(123) = 0.321$. Denoting the ith prime number as $b(i)$, the νth point of a D-dimensional Halton sequence can then be written as $\{\Phi_{b(1)}(\nu),\Phi_{b(2)}(\nu),\ldots,\Phi_{b(D)}(\nu)\}$.

To reduce correlations (esp. in higher dimensions), we use the permutations by Faure [35] to introduce scrambling in the radical inverse function. The permutations σ_b are constructed in an iterative way by starting with $\sigma_1 = (\sigma_1(0)) = (0)$. For even b, σ_b is constructed[7] by taking $2\sigma_{b/2}$ and appending $2\sigma_{b/2}+1$.

For odd b, σ_b is derived from σ_{b-1} by incrementing each value which is $\geq \frac{b-1}{2}$ and inserting $\frac{b-1}{2}$ in the middle. The first permutations consequently are (we omit $\sigma_1 = (0)$)

$$\begin{aligned} &\sigma_2 = (0,1), \qquad \sigma_3 = (0,1,2), \\ &\sigma_4 = (0,2,1,3),\ \sigma_5 = (0,3,2,1,4),\ \ldots \end{aligned}$$

[6] We refer to uniform distributions according to the appropriate Haar measure [26].

[7] Writing $a \times \sigma_b + c$ is a short-hand notation for applying the linear transformation to every element of σ_b, that is multiplying every element by a and then adding c.

The radical inverse function can then be modified to

$$\Phi'_b(\nu) = \sum_{k=0}^{\infty} \sigma_b(\alpha_k) b^{-k-1}. \tag{29}$$

By again denoting the ith prime number as $b(i)$, we can finally assign the scrambled Halton sequence to our parameter vectors via

$$\tilde{\mathcal{P}}^{\nu} = \{\Phi'_{b(1)}(\nu),\Phi'_{b(2)}(\nu),\ldots,\Phi'_{b(D)}(\nu)\}\,. \tag{30}$$

References

1. A. Peres, Am. J. Phys. **52**, 644 (1984)
2. C.W. Helstrom, *Quantum Detection and Estimation Theory* (Academic Press, New York, 1976)
3. A.S. Holevo, *Probabilistic and Statistical Aspects of Quantum Theory* (North-Holland, Amsterdam, 1982)
4. A nice review about quantum state estimation can be found in various chapters of: *Quantum State Estimation*, edited by M.G.A. Paris, J. Řeháček, Lecture Notes in Physics **649** (Springer, Berlin, Heidelberg, 2004)
5. A. Peres, W.K. Wootters, Phys. Rev. Lett. **66**, 1119 (1991)
6. S. Massar, S. Popescu, Phys. Rev. Lett. **74**, 1259 (1995)
7. R. Derka, V. Bužek, A.K. Ekert, Phys. Rev. Lett. **80**, 1571 (1998)
8. J.I. Latorre, P. Pascual, R. Tarrach, Phys. Rev. Lett. **81**, 1351 (1998)
9. D. Bruß, C. Macchiavello, Phys. Lett. A **253**, 249 (1999)
10. G. Vidal, J.I. Latorre, P. Pascual, R. Tarrach, Phys. Rev. A **60**, 126 (1999)
11. D.G. Fischer, S.H. Kienle, M. Freyberger, Phys. Rev. A **61**, 032306 (2000)
12. D.F.V. James, P.G. Kwiat, W.J. Munro, A.G. White, Phys. Rev. A **64**, 052312 (2001)
13. J.J. Longdell, M.J. Sellars, Phys. Rev. A **69**, 032307 (2004)
14. F.A. Bonk, R.S. Sarthour, E.R. deAzevedo, J.D. Bulnes, G.L. Mantovani, J.C.C. Freitas, T.J. Bonagamba, A.P. Guimarães, I.S. Oliveira, Phys. Rev. A **69**, 042322 (2004)
15. F. Embacher, H. Narnhofer, Ann. Phys. (N.Y.) **311**, 220 (2004)
16. Th. Hannemann, D. Reiss, Ch. Balzer, W. Neuhauser, P.E. Toschek, Ch. Wunderlich, Phys. Rev. A **65**, 050303(R) (2002)
17. R.T. Thew, K. Nemoto, A.G. White, W.J. Munro, Phys. Rev. A **66**, 012303 (2002)
18. K.R.W. Jones, Ann. Phys. (N.Y.) **207**, 140 (1991)
19. K.R.W. Jones, Phys. Rev. A **50**, 3682 (1994)
20. Z. Hradil, J. Summhammer, G. Badurek, H. Rauch, Phys. Rev. A **62**, 014101 (2000)
21. S. Weigert, Phys. Rev. A **45**, 7688 (1992)
22. K. Banaszek, G.M. D'Ariano, M.G.A. Paris, M.F. Sacchi, Phys. Rev. A **61**, 010304 (2000)
23. H.F. Hofmann, S. Takeuchi, Phys. Rev. A **69**, 042108 (2004)
24. J. Řeháček, B.-G. Englert, D. Kaszlikowski, Phys. Rev. A **70**, 052321 (2004)
25. A. Peres, *Quantum theory: concepts and methods* (Kluwer Academic Publishers, Dordrecht, 1993); M.A. Nielsen, I.L. Chuang, *Quantum Computation and Quantum Information* (Cambridge University Press, Cambridge, 2000)

26. A. Hurwitz., Nachr. Ges. Wiss. Gött. Math.-Phys. Kl., 71 (1897)
27. K. Życzkowski, H.-J. Sommers, J. Phys. A: Math. Gen. **34**, 7111 (2001)
28. J.H. Shapiro, S.R. Shepard, N.C. Wong, Phys. Rev. Lett. **62**, 2377 (1989)
29. S.L. Braunstein, A.S. Lane, C.M. Caves, Phys. Rev. Lett. **69**, 2153 (1992)
30. Z. Hradil, Phys. Rev. A **55**, R1561 (1997)
31. R. Schack, T.A. Brun, C.M. Caves, Phys. Rev. A **64**, 014305 (2001)
32. See, for example, F.J. Hickernell, A Comparison of Random and Quasirandom Points for Multidimensional Quadrature, *Monte Carlo and Quasi-Monte Carlo Methods in Scientific Computing*, edited by H. Niederreiter, P.J.-S. Shiue, Lecture Notes in Statistics **106** (Springer, New York, 1995)
33. H. Niederreiter, *Random number generation and quasi-Monte Carlo methods* (Society for Industrial and Applied Mathematics, Philadelphia, 1992)
34. J.H. Halton, Num. Math. **2**, 84 (1960)
35. H. Faure, J. Number Theory **42**, 47 (1992)
36. D.J.C. Bures, Trans. Am. Math. Soc. **135**, 199 (1969); A. Uhlmann, Rep. Math. Phys. **9**, 273 (1976)
37. K. Życzkowski, H.-J. Sommers, Phys. Rev. A **71**, 032313 (2005)
38. For a short introduction to the Fubini-Study metric see, for exemple, Appendix A in N. Barros e Sa, J. Math. Phys. **42**, 981 (2001)
39. I.D. Ivanović, J. Phys. A **14**, 3241 (1981)
40. W.K. Wootters, B.D. Fields, Ann. Phys. (N.Y.) **191**, 363 (1989)
41. S. Bandyopadhyay, P.O. Boykin, V. Roychowdhury, F. Vatan, Algorithmica **34**, 512 (2002)
42. G. Kimura, Phys. Lett. A **314**, 339 (2003)
43. G. Kimura, A. Kossakowski, e-print `arXiv:quant-ph/0408014` (2004)
44. W.H. Press, S.A. Teukolsky, B.P. Flannery, W.T. Vetterling *Numerical Recipes in C* (Cambridge University Press, Cambridge, 2002)
45. J.M. Hammersley, Ann. New York Acad. Sci. **86**, 844 (1960)
46. J. Lawrence, Č. Brukner, A. Zeilinger, Phys. Rev. A **65**, 032320 (2002)
47. K. Życzkowski, M. Kuś, J. Phys. A: Math. Gen. **27**, 4235 (1994)